Identifying, quantifying, and determining the root causes of specific spreadability issues with AM powders

Abstract

Powders used in the AM industry either they spread well or they do not. Poor powder spreading is due to specific issues with the powder or printer parameters. Therefore, the specific spreadability issues must be identified and quantified so that the root cause of the issue can be determined and corrected. Data is presented in identifying and quantifying various spreadability issues including low layer density, low layer thickness, non-uniform layer coverage, channeling, and layer waviness. The root causes of these issues are determined, and corrective actions are presented.

Introduction

The ability of a powder to form a layer in a powder AM printer is critical to producing high quality parts. This ability is referred to as powder spreadability. Powders used in AM printing must spread well enough to form a very thin and uniform layer of powder on top of both a loose powder bed and a fused layer of powder. The fused layer of the powder can be due to melting as in laser sintering or due to binder holding the powder together as in binder jetting. The thickness of the powder layer being spread is open to some debate but can be considered to be in the thirty to two hundred micrometer range depending on the type of printing process being used and the type of powder.

Problems with printing arise when powder do not spread well in the printer. These problems include no layer being spread, low layer thickness, low layer density, poor spread layer coverage, channels in the layer, and layer waviness. These problems can start immediately with a powder, can develop as the printing process continues or as the powder is recycled. It is too late to prevent spreadability problems once a printing cycle has started so it is critical to determine a powder's spreadability before printing starts so the powder is not used or corrective actions are taken.

To address this problem a device has been introduced commercially to measure powder spreadability. The SpreadStation Powder Spreadability Analyzer creates up to four simultaneous layers of powder using various spreader geometries, spreader speeds and powder feeding options. The analyzer then measures the quality of the powder layer using optical techniques and by measuring the mass of material exiting the spreader. The analyzer can also measure the static charge on the tested powders after spreading. The test powder can be spread on various build plates or on a powder bed.

1.a: spreadability analyzer

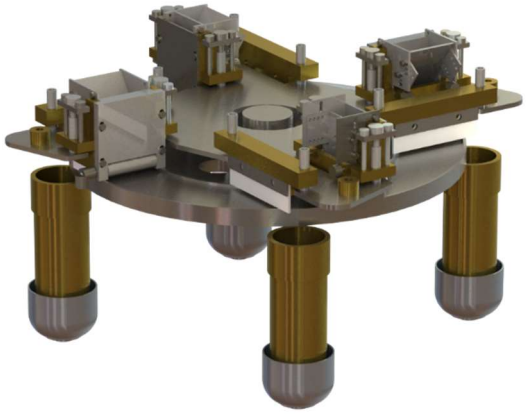

1.b: solid build plate with four spreading assemblies

Figure 1. Spreadability analyzer

For a powder to form a layer on a build plate there must be relative motion between the spreading device and the build plate. In most AM printers the spreading device moves over the build plate to spread the powder. In the powder spreadability analyzer, the build plate is moved under the spreading device to spread the powder. The build plate is rotated relative to the spreading device to keep the system small for controlling environmental conditions and to provide unlimited travel for the build plate [Figure 1]. This simplifies the design of the device and makes it easier to mount measuring systems as they are stationary. After being spread, the powder is removed from the build plate by an angled scraping blade and transferred to a measuring balance to be weighed. The instrument can be equipped with multiple spreaders and balances.

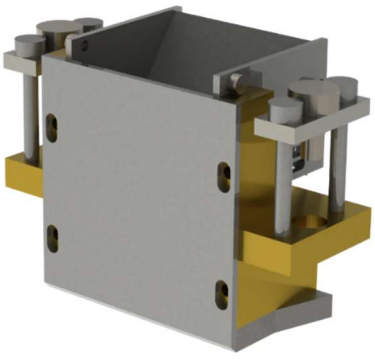

Figure 2. Spreading assembly with spreading base, spreading plate and powder feeder installed

Figure 3. Powder feeder

The spreading assembly [Figure 2] for the analyzer consists of three parts: 1) a spreading base, 2) a spreading plate, and 3) a powder feeder [Figure 3]. The spreading plate is mounted on the spreading base and can move in the vertical direction to create a gap between the build plate and the spreading plate to allow powder to spread. The spreading device moves up and down with any unevenness in the build plate to maintain a constant spreading gap. Many spreading geometries are available including flat, rounded, flexible and counter rotating cylinder. The spreading base maintains the powder behind the spreading plate. The powder feeder delivers the powder to the spreading area. The angle and gap of the feeder can be adjusted as well as the pressure on the powder in the spreading area. Up to four spreading devices can be mounted on the analyzer to spread four layers simultaneously. When the test-powder is loaded in the powder feeder, the movement of the build plate starts and the powder spreads in a layer on the build plate where it is measured.

Several measurements are made to assess the powder layer. The primary measurement is the mass of powder that exits the spreader relative to the motion of the build plate. After exiting the spreading device, the powder is moved off the build plate and onto a balance by an angled scraping blade. The balance measures the mass of powder removed from the build plate over time. Before reaching the blade, images of the powder are taken, and the thickness of the powder bed is measured using a distance sensor. The density of the bed is calculated from the height of the powder or spreading gap and the travel of the build plate. Channels and waves in the powder layer are detected using image analysis techniques on the powder images.

These measurements allow layer uniformity and allow density to be measured over the course of the spreading until no more powder exits the spreading device. The spreading efficiency is the spreading density of the layer relative to a layer of solid powder material at the thickness of the spreading gap. The spreading rate is the mass of powder in the layer per centimeter traveled by the build plate. The standard deviation of the spreading rate is the standard deviation of the mass of the powder being spread taken every one second. The spread uniformity compares the spreading rate at the beginning of the measurement and at the end of the measurement to the average spread rate. A uniformity of zero means there is no variation in the spreading rate. A negative uniformity means less powder is being spread at the end of the test as compared to the beginning. A positive uniformity means more powder is being spread at the beginning of the test than at the end. The fractal dimension is the smoothness of the mass in the spread layer.

The spreadability tester can identify and quantify specific powder spreadability issues like poor layer coverage, channeling, waviness, etc. But the reasons for these behaviors need to be identified and corrective actions need to be taken to prevent poor printing runs. The most expensive corrective action is not to use the powder if it has poor spreadability. Other corrective actions include processing the powder in some way to change powder variables or changing the printer variables. The variables available for both the printer and powders are presented in Table 1. In this paper several scenarios will be presented that identify and quantify specific spreadability problems and then present corrective actions to reduce or eliminate the problem.

Table 1: Variables in AM applications

Printing Variables	**Material Variables**
Leveling Height	Particle Size and Distribution
Spreader Speed	Flowability
Spreader Geometry	Particle Shape
Pressure on the Powder	Surface and Moisture Properties
Powder Feeding System	Static Charge
Environmental Conditions in the printer	Segregation

Unlike real applications, the material variables were imposed on the samples before testing so that the conditions of the powder were known. This is to demonstrate the effect of a specific change in the sample. In real applications, the powder spreads poorly and the reason must be determined. This can sometimes be deduced from the spreadability data itself or it may require additional testing. Additional testing can involve re-testing the spreadability under the same or different conditions viz. test the flowability of the samples, or dry the sample, or remove static of the samples.

To compare the spreadability of a powder to the flowability of the powder, the flow properties of the powders were characterized with the Revolution Powder Analyzer which is very sensitive to small changes in AM powders. The analyzer has demonstrated the capability to capture differences in 316L stainless steel powders atomized by argon or nitrogen [1]. The argon atomized powder consistently displayed better flowability than the nitrogen atomized powders measured by flow test using the analyzer. These differences in flowability of the powders were correlated to the powder morphology, with argon atomized powder displaying higher sphericity. Differences in flowability of virgin and recycled 304L stainless steel powders were also identified using the Revolution tool [2]. After 7 uses, both the PSD and particle shape changed, which resulted in the different flow properties of the recycled powder. Elemental powders, Fe and Ni, were tested using the analyzer concerning their flow properties [3]. With different PSD and particle shape, the powders displayed different flow properties, which were successfully captured by the Revolution tool.

This paper is a companion paper to [4] and [5] which contain the full details of the spreadability and flowability measurements of the samples.

Materials

One set of two 316L austenitic stainless steel powder samples labeled as Set A were tested. The set consisted of a virgin sample and a recycled version of the same material where the recycled material went through two printing cycles. This material was characterized extensively in [6] and [7] using various measurements including SEM images.

One 316L austenitic stainless steel SLS powder 23-50 µm labeled as Sample B

One set of nickel alloy powders were tested consisting of a virgin material and a recycled material labeled Set C. The virgin material was reported to be acceptable and the recycled material unacceptable for an AM printing application.

Experimental

Measurements of powder spreadability were made using the SpreadStation Powder Analyzer from Mercury Scientific (Newtown, CT). The analyzer was equipped with a flat spreading plate with spreading gaps from fifty to two hundred micrometers. Powders were tested at spreader speeds from fifty to two hundred millimeters per second. The analyzer was equipped with a machine vision camera and LED lighting to capture images of the spread powders and a laser triangulation distance sensor to measure spread layer thickness. The analyzer was also equipped with a field meter to measure static charge on the sample powder.

The low-pressure powder feeder used had a feed angle of 60 degrees and a feeding gap of 4.6 millimeters. The build plate consisted of a stainless-steel disc.

For all tests, 40 grams or roughly 10 cm^3 of sample were tested for each test. Test time was 30 to 50 seconds from the start of spreading to the end of spreading. The total travel of the spreading assemblies was 200 to 300 centimeters which is equivalent to a 2 to 3 meter long build plate.

Spreader bases and powder feeders were removed and wiped with a dry towel to clean them between samples. The build plate was rotated for 200 cm at 50 millimeters per second to clean it for the next test. This required 33 seconds.

The flowability of the samples were tested using the Revolution Powder Analyzer, which utilizes a rotating drum with transparent sides to measure the flowability static charging of powders. During the tests, a powder volume of 25 cm^3 or 100 cm^3 was loaded into the drum. As the drum was rotated on a pair of motor-driven rollers at pre-defined rotation rates, the avalanche profile of the powders was captured using a digital camera, with the assistance of LED back-light illumination, as shown in Figure 1. The images of the avalanche profile were collected and processed at 20 frames per second to capture the exact motion of the powder sample. From the images collected, image analysis was then conducted, and numerous parameters were measured or calculated. A reference mask allows for calibration of the imaging system. Several testing modes are available on the Revolution Powder Analyzer, which include flow, packing, and multi-flow and static charging tests [8]. Each of the tests examines a unique aspect of powder properties. The powders in this case were tested with the flow and static charge tests.

Figure 4. Illustration of working principle of Revolution Powder Analyzer. Avalanche profile of powders is captured by a camera as the drum is rotating. The avalanche angle α is measured by image analysis

In the flow test, a relatively low rotation rate of 0.3 rotations per minute (rpm) is used, and the details on the avalanche behaviors are captured. The instrument captures 100 avalanches and provides averaged results. Flow properties of the powder can be evaluated by measuring the avalanche angles, which are captured by the camera when the powder avalanche begins. The break energy represents the maximum energy level of the powder test portion before an avalanche begins. The avalanche energy is the amount of energy released during an avalanche. The dynamic density can be calculated from the measured mass of the powder and the bulk volume determined using image analysis tools as the drum is rotating. The cohesion-T is the average of the shear stress overcome by the flowing layer as the powder moves during avalanche.

All samples were tested in as is condition. Sample A Recycled was exposed to humidity by placing it in an open pan in an oven with a relative humidity of 40 percent and a temperature of 50 degrees Celsius for two hours with mixing every 30 minutes to expose additional surfaces to the oven humidity. The sample was then tested. After testing the sample was dried at 100 degrees Celsius for 16 hours and then at 200 degrees Celsius for two hours with mixing every 30 minutes. The sample was then cooled and tested again.

Set A Recycled was also exposed to segregation stress using a pan sifting method. 100 cm^3 of the sample was transferred to a flat pan. The pan was shaken from side to side for 60 seconds to create a motion in the sample. The top half of the sample was then scraped from the powder bed and collected. Then the lower layer was collected. Each pan layer was then tested.

Results and Discussion

The spread layer thicknesses used in this study were selected to match the effective layer thickness of the powder layers in a typical fusion powder bed AM printer. This effective layer thickness has been measured to be five to ten times the leveling height of the build platform [9,10]. For a typical twenty or thirty micrometer leveling height the effective layer thickness over the printed parts is 100 to 200 micrometers [9,10]. The leveling height on a printer is the amount of vertical movement of the spreader for each layer and is typically a constant value. The gap between the spreader and the part surface is not constant and depends on the thickness of the melt pool of the material and the thickness of the previous layer of powder. A feedback loop exists between the spreading gap and the actual thickness of the current and previous powder layer. If the current layer is thinner than the previous layer, then the next layer will have a larger spreading gap which in turn should create a thicker powder layer. If the current layer is thicker than the previous layer, then the spreading gap will be smaller for the next layer. This is also true for the density of the powder layer. A denser layer will form a thicker melt pool which will create a smaller spreading gap in the next layer and vice versa.

The effective layer thickness is also obviously influenced by the size and size distribution of the powder particles, the shape of the powder particles, the flowability of the powder, the static charge on the particles, etc. For example, a 50 micrometer particle cannot move through a gap less than 50 micrometers. Powder particles also do not form a monolayer of particles in a powder layer. Therefore, the true layer thickness of powder particles over a part or powder bed will be larger than the leveling height of the printer and will be affected by the powder and printer properties.

For the flow measurements, a low drum speed for the testing has been used for two reasons. One reason is that the speed of the particles in the powder bed in the spreading area of typical printers has been observed to be low for many printers. The other reason is that low speed tests are more sensitive to small changes in the test powder. This is derived from 20 years of testing with the instrument. Low speed tests emphasize particle to particle interactions in the powder as opposed to higher speeds which are more about the dilation of the powder bed due to higher particle velocity and aeration.

Scenario 1: Good Spreadability

A summary of the spreadability data for Set A Virgin and Recycled samples with a flat spreading plate, a spreading gap height of 150 micrometers and spreading speeds of 50 millimeters per second is given in Table 2. Layer heights for the spread layer are given in Table 3. Images of the spread layer are given in Figure 5.

Table 2. Summary of the spreadability data for Set A samples tested with a flat spreading plate, a 150 µm spreader gap and a spreading speed of 50 mm/s

Sample	Spread Eff. %	Layer Density g/cm^3	Spread Rate mg/cm	Spread Rate SD mg/cm	Spread Unif. %	Fractal Dim.
Set A Virgin	49.3	3.95	206	8	0.8	3.07
Set A Recycled	49.8	3.99	208	11	-7.7	2.76

Table 3. Summary of the measured layer thickness for Set A samples tested with a flat spreading plate, a 150 micrometer spreader gap and a spreading speed of 50 mm/s

Sample	Measured layer thickness µm	Measured Layer Density g/cm^3	Measured Spread Efficiency %
Set A Virgin 50 mm/s	158	3.75	46.9
Set A Recycled 50 mm/s	171	3.49	43.7

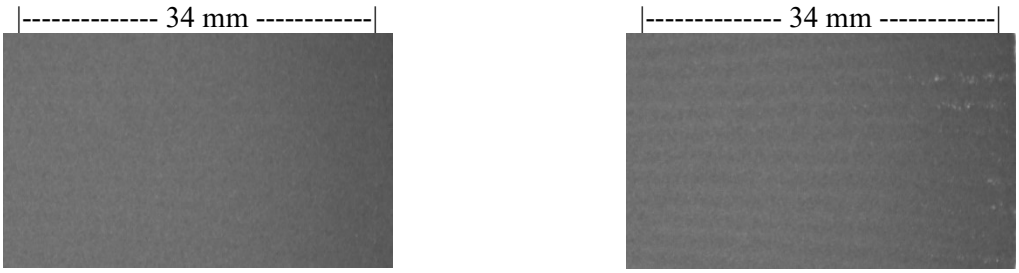

5.a: Set A Virgin 50 mm/s

5.b: Set A Recycle 50 mm/s

Figure 5. Images of Set A samples tested with a flat spreading plate, a 150 µm spreader gap and 50 mm/s

When powder is spreading well, the spreading efficiency is typically above 40%. In this case both powders have a spreading efficiency of 49% and it is uniform from the beginning to the end of the test. This means that the spread layer density is close to the bulk density of the sample powder. Good spreadability is also indicated by the powder layer thickness being near the leveling height set by the gap in the spreader. In this case the spread layer thickness is slightly higher than the spreader gap. Good spreadability is also indicated by a smooth powder layer as shown in the images of the powder layer. Analyzing the images shows that there are no gaps in the powder layer coverage, no channels and no waves. Image analysis data is presented in Table 4.

Table 4. Summary of the image analysis data for Set A samples tested with a flat spreading plate, a 150 micrometer spreader gap and a spreading speed of 50 mm/s

Sample	Area Coverage %	Channels width mm	Waves %
Set A Virgin 50 mm/s	100%	0	0
Set A Recycled 50 mm/s	100%	0	0

Scenario 2: Poor Spreadability After Recycling Root Cause Flowability

A summary of the spreadability data for Set C Virgin and Recycled samples with a flat spreading plate, a spreading gap height of 150 micrometers and spreading speeds of 50 millimeters per second is given in Table 5. Layer heights for the spread layer are given in Table 6. Images of the spread layer are given in Figure 6.

Table 5. Summary of the Spreadability data for Set C samples tested with a flat spreading plate, a 150 µm spreader gap and a spreading speed of 50 mm/s

Sample	Spread Eff. %	Layer Density g/cm^3	Spread Rate mg/cm	Spread Rate SD mg/cm	Spread Unif. %	Fractal Dim.
Set C Virgin	43.4	3.47	182	9	-1.8	3.16
Set C Recycled	28.6	2.45	130	10	3.6	5.00

Table 6. Summary of the measured layer height for Set C samples with a flat spreading plate, a 150 µm spreader gap and a spreading speed of 50 mm/s

Sample	Measured layer thickness µm	Measured Layer Density g/cm^3	Measured Spread Efficiency %
Set C Virgin	132	3.94	45.9
Set C Recycled	73	5.02	58.4

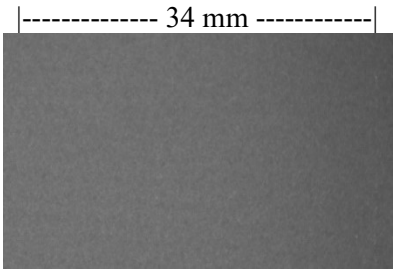

6.a: Set C Virgin 50 mm/s

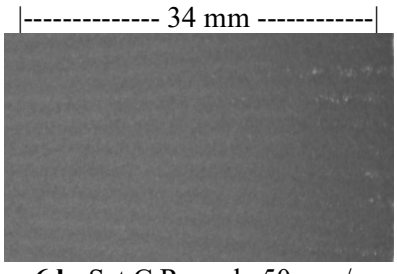

6.b: Set C Recycle 50 mm/s

Figure 6. Images of Set C samples tested with a flat spreading plate, a 150 µm spreader gap and multiple speeds

In this case the virgin powder has a spreading efficiency of 43% and the recycled powder has a spreading efficiency of 29%. The recycled powder also has a layer thickness that is roughly half of the leveling height set by the gap in the spreader. The images show that both the virgin and recycled powders produced a fairly smooth powder layer but the recycled material had some waviness. Analyzing the images shows that there are no gaps in the powder layer coverage and no channels. Image analysis data is presented in Table 7. This means that the problem with the recycled layer is simply that it is too thin but has a reasonable density.

Table 7. Summary of the image analysis data for Set C samples tested with a flat spreading plate, a 150 micrometer spreader gap and a spreading speed of 50 mm/s

Sample	Area Coverage %	Channels width mm	Waves mm
Set C Virgin	100%	0	0
Set C Recycled	100%	0	0.5

Table 8 shows the flowability data for the Set C samples. The recycled sample has much poorer flowability than the virgin sample. The cause of this change in flowability was not identified in this case. The usual corrective action for poor flow after recycling is to mix in a percentage of virgin powder to refresh the powder. The flow of a 50% blend improved the flow to where it is between the Virgin and Recycled material.

Table 8. Summary of the flowability data for Set C samples

Sample	Avalanche Energy mJ/kg	Avalanche. Angle deg	Cohesion-T Pa	Dynamic Density g/ cm^3	Volume Fraction
Set C Virgin As Is	14.7	41.5	80.7	4.30	0.551
Set C Recycled As Is	24.9	50.9	194.5	3.82	0.489
Set C Blend	20.6	46.7	118.8	4.38	0.561

Scenario 3: Poor Spreadability Root Cause Increased Moisture Content

A summary of the spreadability data for Set A Recycled sample with humidity exposure followed by drying using a flat spreading plate, a spreading gap height of 150 micrometers and spreading speeds of 50 millimeters per second is given in Table 9. Sample A Recycled Humid was exposed to moisture in a humidity oven and Sample A Recycled Dried was the humid sample dried in an oven.

Table 9. Summary of the Spreadability data for Set C samples tested with a flat spreading plate, a 150 µm spreader gap and a spreading speed of 50 mm/s

Sample	Spread Eff. %	Layer Density g/cm^3	Spread Rate mg/cm	Spread Rate SD mg/cm	Spread Unif. %	Fractal Dim.
Set A Recycled Humid	40.4	3.23	170	10	-11.5	3.55
Set A Recycled Dried	45.4	3.63	191	11	-7.4	3.16
Set A Recycled Typical	49.8	3.99	208	11	-7.7	2.76

The sample exposed to humidity had poorer spreadability as compared to the typical sample with lower spreading efficiency and layer density. The issue of creating the poor spreadability was poor flowability. This can be seen in the flow data from the powder flow analyzer as presented in Table 10. For humid recycled powder all of the avalanche energy, avalanche angle, and cohesion were increased. The dynamic density did not decrease, however, as is usual when a powder has poorer flow. This pattern is typical when the moisture content increases in a powder. The weight of the moisture compensates somewhat for the increased gaps in the powder bed due to poorer flow. Drying the powder improved the spreadability and flow indicating that moisture uptake was the root cause of the problem. The corrective action for the powder is to bake the material to drive off the excess moisture.

Table 10. Ranking of the flowability of humidity exposed Set A and Set B samples ranked by Avalanche Angle

Sample	Avalanche Energy mJ/kg	Avalanche. Angle deg	Cohesion-T Pa	Dynamic Density g/ cm^3	Volume Fraction
Set A Recycled Humid	19.71	46.3	97.04	4.227	0.528
Set A Recycled Dry	13.05	34.3	35.32	4.382	0.547
Set A Recycled Typical	17.70	36.5	90.63	4.234	0.529

Scenario 4: Poor Spreadability – Root Cause Large Particles

A summary of the spreadability data for Set A Recycled sample after pan segregation using a flat spreading plate, a spreading gap height of 150 micrometers and spreading speeds of 50 millimeters per second is given in Table 11. Sample A Recycled Large Particles is the top pan cut which contained more oversized particles from the sample. Sample A Recycled Less Large Particles is the bottom pan cut which contained less oversized particles from the sample. Images of the spread layer are given in Figure 7.

Table 11. Summary of the spreadability data for Set A Recycled pan segregated samples tested with a flat spreading plate, a spreading gap of 150 µm and a spreading rate of 50 mm/s

Sample	Spread Eff. %	Layer Density g/cm^3	Spread Rate mg/cm	Spread Rate SD mg/cm	Spread Unif %	Fractal Dim.
Set A Recycled Large Particles	38.1	3.05	159	19	-24.6	3.75
Set A Recycled Less Large Particles	53.7	4.30	224	11	-5.4	2.23

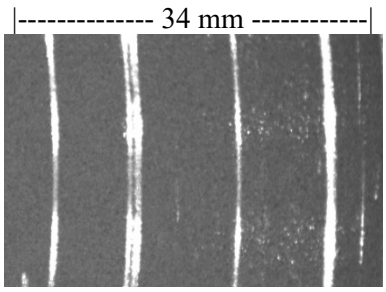

7.d: Set A Recycle Large Particles

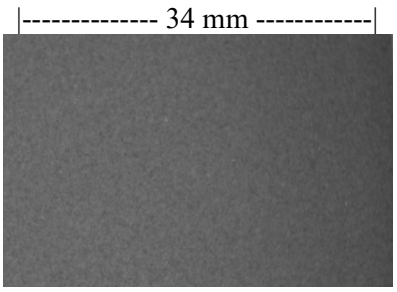

7.b: Set A Recycle less Large Particles

Figure 7. Images of Set A Recycled pan segregated samples tested with a flat spreading plate, a spreading gap of 150 µm and a spreading rate of 50 mm/s

The sample with large particles present had poor spreadability as indicated by the low spreading efficiency and layer density. The images of the powder layer show large channels in the spread powder layer. Channels are typically produced by large particles blocking the spreading of particles from the recoater because they are too large to pass between the recoated and the part surface. The channels in the layer are reducing the amount of coverage of the powder in the layer to 86 percent as seen in the image analysis data in Table 12. Removing a percentage of the large particle by pan sifting improved the

spreading and eliminated the channels indicating that the large particles were the root cause of the problem. This is also verified by the fact that the flowability of the powder did not change when the large particles were reduced as seen in the flowability data presented in Table 13. The corrective action is to screen out the large particles. Areas of high concentration of large particles can also be caused by segregation of the powder. This can be detected by testing the spreadability of samples of the powder from different locations. If only certain areas of the sample create channels in the powder bed, then the corrective action is to remix the powder.

Table 12. Summary of the image analysis data for Set A Recycled samples after pan sifting with a flat spreading plate, a 150 micrometer spreader gap and a spreading speed of 50 mm/s

Sample	Area Coverage %	Channels	Channel width mm	Waves %
Set A Recycled Large Particles	86.3%	4	0.79	0
Set A Recycled Less Large Particles	100%	0	0	0

Table 13. Summary of the flow data for each sample

Sample	Avalanche Energy mJ/kg	Avalanche Angle deg	Cohesion-T Pa	Dynamic Density g/cc	Volume Fraction
Set A Recycled Large Particles	8.6	36.9	40.1	4.402	0.550
Set A Recycled Less Large Particles	7.8	36.1	34.8	4.279	0.534

Scenario 5: Poor Spreadability Root Cause Static

A summary of the spreadability data for Set 316L sample with static exposure and rest time exposure using a flat spreading plate, a spreading gap height of 200 micrometers and spreading speeds of 50 millimeters per second is given in Table 14. Sample 316L Static was exposed to static by tribocharging with Teflon and Sample 316L Rested after Static was the static sample sitting for 13 minutes to allow the static charge to dissipate.

Table 14. Summary of the Spreadability data for Set A Virgin samples with a flat spreading plate, a 150 µm spreader gap and a spreading speed of 50 mm/s

Sample	Spread Efficiency %	Layer Density g/cm^3	Spread Rate mg/cm	Spread Uniformity %	Surface charge V
Sample B with Static	34.9	2.80	192	-49.3	490
Sample B Rested after Static	42.1	3.38	229	-22.2	155
Sample B Typical	57.5	4.61	303.7	-8.5	10

The static charge on the sample caused the spreadability to be poor. The static on the powder also caused the voltage on the collector cup of the spreading machine to have a high voltage. By letting the sample rest the static dissipated reducing the voltage on the cup and improving the spreadability. Samples can also be tested for static by exposing them to air from a de-ionizing blower. The blower eliminates static on the surface of the powder particles. After static removal the sample can be re-tested to determine if the spreadability improves. The corrective action for static is to let the powder sit for a period of time until the static naturally dissipates.

Scenario 6: Poor Spreadability Root Cause Spreading Speed Too Fast

A summary of the spreadability data for Set A Virgin samples tested with a flat spreading plate, a spreading gap height of 150 micrometers and spreading speeds of 200, 150, 100 and 50 millimeters per second is given in Table 15. Images of the spread layer are given in Figure 8.

Table 15. Summary of the spreadability data for Set A samples tested with a flat spreading plate, a 150 µm spreader gap and multiple speeds

Sample	Spread Eff. %	Layer Density g/cm^3	Spread Rate mg/cm	Spread Rate SD mg/cm	Spread Unif. %	Fractal Dim.
Set A Virgin 200 mm/s	22.8	1.83	94	6	5.7	7.01
Set A Virgin 150 mm/s	31.4	2.51	129	9	6.2	5.16
Set A Virgin 100 mm/s	38.3	3.06	157	5	17.5	4.22
Set A Virgin 50 mm/s	49.3	3.95	206	8	0.8	3.07

The data indicates that the spreading efficiency calculated from the spreading gap height drops with spreading speed. The spread rate is also less uniform at faster spreading rates as evidenced by the increasing fractal dimension. Table 16 presents the measured layer thickness and measured layer density for the data set in Table 15.

Table 16. Summary of the measured layer thickness for Set A samples tested with a flat spreading plate, a 150 micrometer spreader gap at multiple speeds

Sample	Measured layer thickness µm	Measured Layer Density g/cm^3	Measured Spread Efficiency %
Set A Virgin 200 mm/s	72	3.82	47.8
Set A Virgin 150 mm/s	100	3.78	47.2
Set A Virgin 100 mm/s	117	3.92	48.9
Set A Virgin 50 mm/s	158	3.75	46.9

The thickness of the spread layer decreases below the spreading gap height at speeds above 50 mm/s. This reduces the spreading efficiency calculated from the spreading gap height as the powder layer is no longer being spread at the gap height. However, the measured layer density remains relatively constant across all the spreading speeds. The powder layer that is spread has a consistent density with increasing speed even though the thickness of the layer is decreasing as the spreading speed increases. The implication of this is that these powders will spread uniformly at faster spreading speeds but the melt pool thickness will decrease with increased speed.

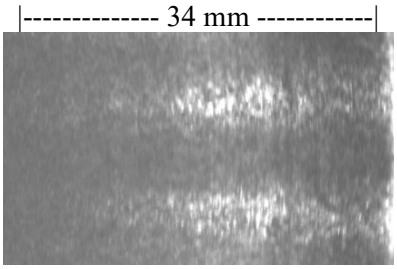

8.a: Set A Virgin 200 mm/s

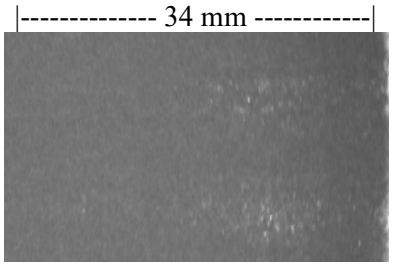

8.b: Set A Virgin 150 mm/s

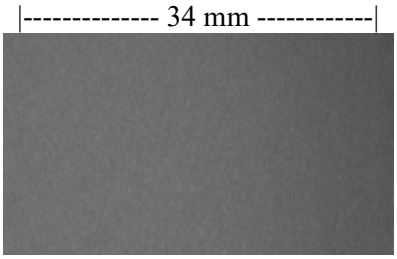

8.c: Set A Virgin 100 mm/s

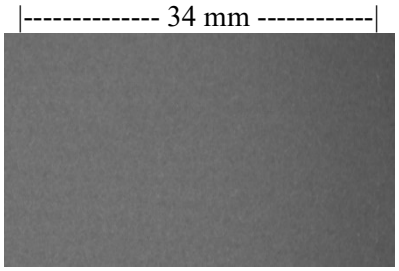

8.d: Set A Virgin 50 mm/s

Figure 8. Images of Set A samples tested with a flat spreading plate, a 150 µm spreader gap and multiple speeds

Table 17. Summary of the image analysis data for Set A samples with a flat spreading plate, a 150 micrometer spreader gap and a spreading speed of 50 mm/s

Sample	Area Coverage %	Channels	Channel width mm	Waves %
Set A Virgin 200 mm/s	77	0	0	0
Set A Virgin 150 mm/s	96	0	0	0
Set A Virgin 100 mm/s	100	0	0	0
Set A Virgin 50 mm/s	100	0	0	0

The image analysis data presented in Table 17 indicates that 200 mm/s is too fast to get complete powder coverage of the build plate. The coverage is better at 150 mm/s.

Scenario 7: Poor Spreadability Root Cause Spreading Gap Too Low

A summary of the spreadability data for Set A Recycle sample tested with a flat spreading plate, a spreading speed of 50 mm/s and spreading gap heights of 50, 100, 150 and 200 micrometers is given in Table 18. Images of the spread layer are given in Figure 8.

Table 18. Summary of the spreadability data for Set A Recycled sample tested with a flat spreading plate, spreading speed of 50 mm/s and multiple spreader gaps

Sample	Spread Eff. %	Layer Density g/cm^3	Spread Rate mg/cm	Spread Rate SD mg/cm	Spread Unif. %	Fractal Dim.
Set A Recycled 50 µm gap	42.8	3.42	60	8	-16.3	5.63
Set A Recycled 100 µm gap	48.3	3.86	136	9	-8.4	2.75
Set A Recycled 150 µm gap	49.8	3.99	208	11	-7.7	2.76
Set A Recycled 200 µm gap	56.7	4.54	318	11	2.6	2.39

The data indicates that the spreading efficiency calculated from the spreading gap height increases with spreading gap height. The spread rate is also more uniform at larger spreading gap heights as evidenced by the decreasing fractal dimension. Table 19 presents the measured layer thickness and measured layer density for the data set in Table 18.

Table 19. Summary of the measured layer thickness for Set A Recycled samples tested with a flat spreading plate, a 50 mm/s spreader speed and multiple spreader gaps.

Sample	Measured layer thickness µm	Measured Layer Density g/cm^3	Measured Spread Efficiency %
Set A Recycled 50 µm gap	35*	*	*
Set A Recycled 100 µm gap	110	3.51	43.9
Set A Recycled 150 µm gap	171	3.49	43.7
Set A Recycled 200 µm gap	214	4.24	53.0

*sample too uneven to measure accurately

The thickness of the spread layer is at or slightly above the spreading gap height for all of the gaps tested except the 50 µm gap. The measured layer density increases with spreading gap height. The images in Figure 9 and the image analysis data in Table 20 show that a 50 µm gap is too small to get complete powder coverage of the build plate.

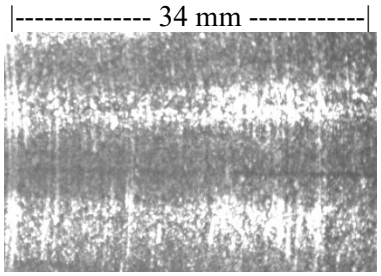

9.a: Set A Recycle 50 µm spreading gap

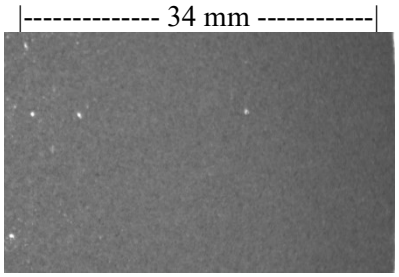

9.b: Set A Recycle 100 µm spreading gap

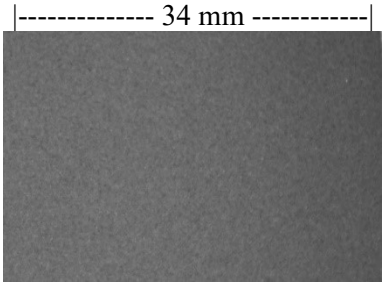

9.c: Set A Recycle 150 µm spreading gap

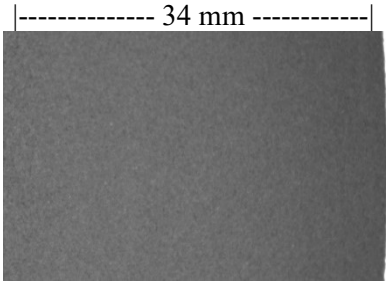

9.d: Set A Recycle 200 µm spreading gap

Figure 9. Images of Set A Recycle samples tested with a flat spreading plate, spreading speed of 50 mm/s and multiple spreader gaps

Table 20. Summary of the image analysis data for Set A samples with a flat spreading plate, a 150 micrometer spreader gap and a spreading speed of 50 mm/s

Sample	Area Coverage %	Channels	Channel width mm	Waves %
Set A Recycled 50 gap	46	0	0	0
Set A Recycled 100 gap	99	0	0	0
Set A Recycled 150 gap	100	0	0	0
Set A Recycled 200 gap	100	0	0	0

Summary and Conclusions

The spreadability and flowability of several metal AM powders were tested using the SpreadStation Powder Spreadability Analyzer and the Revolution Powder Analyzer. The results indicate that good spreadability and spreadability problems can be easily identified and quantified with the spreadability analyzer. In some case the spreadability data alone is enough to determine the root cause of the spreadability problem. For example, oversized particles in a sample create channels in the powder bed and static on a sample creates poor spreadability and a measurable electric field in the sample collection cup. In other cases, sample conditioning and additional testing are required to determine the cause of the problem. For example, baking a sample to drive off excess humidity is needed to determine if moisture content is creating a flow problem that leads to poor spreadability. Some spreadability problems are caused by printer setting which are simply revealed by changing the settings.

References

[1] M.Z. Gao, B. Ludwig, T.A. Palmer, Impact of atomization gas on characteristics of austenitic stainless steel powder feedstocks for additive manufacturing, Powder Technol. In press (2020). https://doi.org/10.1016/j.powtec.2020.12.005.

[2] A.T. Sutton, C.S. Kriewall, S. Karnati, M.C. Leu, J.W. Newkirk, Characterization of AISI 304L stainless steel powder recycled in the laser powder-bed fusion process, Addit. Manuf. 32 (2020) 100981. https://doi.org/10.1016/j.addma.2019.100981.

[3] A.B. Spierings, M. Voegtlin, T. Bauer, K. Wegener, Powder flowability characterisation methodology for powder-bed-based metal additive manufacturing, Prog. Addit. Manuf. 1 (2016) 9–20. https://doi.org/10.1007/s40964-015-0001-4.

[4] Martiska, Greg, Paper 135, Evaluating the spreadability of metal powders for additive manufacturing applications using a new powder spreadability analyzer, presented during Session A17, AMPM 2021 Conference, Orlando, FL.

[5] Martiska, Greg, Paper 137, Evaluating the changing sensitivity of AM powders to segregation and humidity as they are used and recycled, presented during Session A03, AMPM 2021 Conference, Orlando, FL.

[6] Thornton, Particle Size and Shape Evaluation of SS-316L Powders from Interlaboratory Study, IJPM,Vol56, No 4,2020,pp41-57

[7] Saad, Jack G, and Thornton, Tony, Paper 097 presented during Session 22, AMPM 2018 Conference, San Antonio, TX.

[8] Mercury Scientific, Revolution Powder Analyzer User Manual, (2010) 248.

[9] Yahya Mahmoodkhani1 Usman Ali, Shahriar Imani Shahabad, Adhitan Rani Kasinathan, Reza Esmaeilizadeh, Ali Keshavarzkermani, Ehsan Marzbanrad, Ehsan Toyserkani ,On the measurement of effective powder layer thickness in laser powder-bed fusion additive manufacturing of metals, Progress in Additive Manufacturing (2019) 4:109–116

[10] Tim Marten Wischeropp, Claus Emmelmann, Milan Brandt, Aaron Pateras, Measurement of actual powder layer height and packing density in a single layer in selective laser melting, Additive Manufacturing Volume 28, August 2019, Pages 176-183